

Impact of Terrestrial Neutrons on the Reliability of SiC VD-MOSFET Technologies

C. Martinella¹, Member, IEEE, R. G. Alia², Member, IEEE, R. Stark³, Student Member, IEEE, A. Coronetti¹, Member, IEEE, C. Cazzaniga⁴, Member, IEEE, M. Kastriotou⁵, Member, IEEE, Y. Kadi⁶, Member, IEEE, R. Gaillard, Senior Member, IEEE, U. Grossner⁷, Member, IEEE, and A. Javanainen⁸, Member, IEEE

Abstract—Accelerated terrestrial neutron irradiations were performed on different commercial SiC power MOSFETs with planar, trench, and double-trench architectures. The results were used to calculate the failure cross sections and the failure-in-time (FIT) rates at sea level. Enhanced gate and drain leakage were observed in some devices which did not exhibit a destructive failure during the exposure. In particular, a different mechanism was observed for planar and trench gate MOSFETs, the first showing a partial gate rupture with a leakage path mostly between the drain and the gate, similar to what was previously observed with heavy ions, while the second exhibiting a complete gate rupture. The observed failure mechanisms and the postirradiation gate stress (PIGS) tests are discussed for different technologies.

Index Terms—Gate damage, neutrons, power MOSFETs, silicon carbide (SiC), single-event burnout (SEB), single-event effects (SEEs).

I. INTRODUCTION

WIDE-BANDGAP materials such as silicon carbide (SiC) and gallium nitride (GaN) have gained popularity in recent years. Between them, SiC is the most

Manuscript received January 14, 2021; revised January 24, 2021, February 6, 2021, and February 18, 2021; accepted February 22, 2021. Date of publication March 10, 2021; date of current version May 20, 2021. This work was supported in part by the European Space Agency ESA/ESTEC under Contract 4000124504/18/NL/KML/zk and in part by the European Union's Horizon 2020 Research and Innovation Programme under the MSC Grant 721624.

C. Martinella is with the Department of Physics, University of Jyväskylä, 40014 Jyväskylä, Finland, also with the Engineering Department, CERN, 1211 Geneva, Switzerland, and also with the Advanced Power Semiconductor Laboratory (APS), ETH Zurich, 8092 Zurich, Switzerland (e-mail: corinna.martinella@cern.ch).

R. G. Alia and Y. Kadi are with the Engineering Department, CERN, 1211 Geneva, Switzerland (e-mail: ruben.garcia.alia@cern.ch; yacine.kadi@cern.ch).

R. Stark and U. Grossner are with the Advanced Power Semiconductor Laboratory (APS), ETH Zurich, 8092 Zurich, Switzerland (e-mail: stark@aps.ee.ethz.ch; ulrike.grossner@ethz.ch).

A. Coronetti is with the Department of Physics, University of Jyväskylä, 40014 Jyväskylä, Finland, and also with the Engineering Department, CERN, 1211 Geneva, Switzerland (e-mail: andrea.coronetti@cern.ch).

C. Cazzaniga and M. Kastriotou are with the ISIS Facility, STFC, Rutherford Appleton Laboratory, Didcot OX11 0QX, U.K. (e-mail: carlo.cazzaniga@stfc.ac.uk; maria.kastriotou@stfc.ac.uk).

R. Gaillard is Consultant with Saint-Arnoult en Yvelines France (e-mail: remi-gaillard@orange.fr).

A. Javanainen is with the Department of Physics, University of Jyväskylä, 40014 Jyväskylä, Finland, and also with the Electrical Engineering and Computer Science Department, Vanderbilt University, Nashville, TN 37235 USA (e-mail: arto.javanainen@jyu.fi).

Color versions of one or more figures in this article are available at <https://doi.org/10.1109/TNS.2021.3065122>.

Digital Object Identifier 10.1109/TNS.2021.3065122

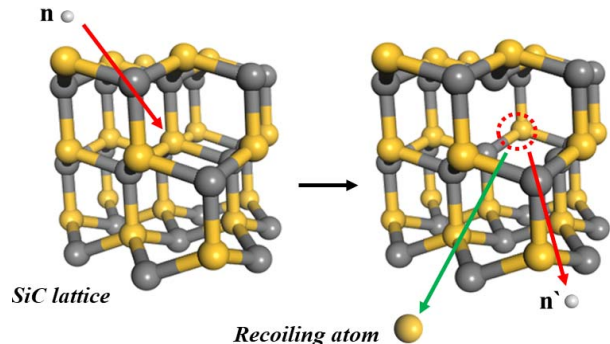


Fig. 1. By the elastic and inelastic scattering with the 4H-SiC lattice, the atmospheric neutrons produce recoiling atoms (i.e., α , C, Si, Mg, and Al) which generate ionizing tracks inside the power MOSFET.

mature technology and has become a viable alternative to silicon-based power devices in high-efficiency and high-power density applications [1], [2]. The higher breakdown field and thermal conductivity make SiC a very attractive material for different ground applications, such as automotive and solar inverters, but also for the avionic and space industries [3], [4]. Moreover, SiC is considered as a promising technology for accelerator applications [5], [6]. However, SiC devices are known to be susceptible to single-event burnout (SEB), single-event gate rupture (SEGR), and single-event leakage current (SELG). SEB and SEGR are caused, among others, by high-energy neutrons [7]–[15], while SELG has been reported only with heavy ions [16]–[20].

The high-energy neutrons originate from cosmic-ray interactions with the atmosphere. These include solar event particles (SEPs) originated by dynamic solar activity and galactic cosmic rays (GCRs) created by events outside the solar system, such as the explosion of galactic nuclei and supernova, pulsars, and stellar flares [21]–[23]. These particles (i.e., 92% protons, 6% alpha particles, and 2% heavier atomic nuclei) are responsible for single-event effects (SEEs) observed in electronics used in space. The particles that are not deviated or trapped by the magnetic field enter the Earth's atmosphere and, upon interacting with, for example, oxygen and nitrogen atoms, create a shower of secondary particles. These interactions result in neutrons, protons, muons, pions, and electromagnetic waves [22]. Some particles decay or are absorbed, while others travel further in the atmosphere, causing a cascade through spallation reactions. Due to the charge neutrality and

TABLE I
LIST OF DUTs

Reference	Man.	$R_{DS(on)}$ [m Ω]	V_{DS} [kV]	$I_{D@25}$ [A]	BV_{DSS} [kV]	Gate	#DUTs
C2M0025120D	Cree/ Wolfspeed	25	1.2	250	1720	planar	51
SCT3030KL	Rohm	30	1.2	180	1926	double trench	48
MSC025SMA120B	Microsemi	25	1.2	275	1586	planar	50
SCTWA50N120	ST-Micr.	59	1.2	130	1520	planar	66
IMW120R090M1H	Infineon	90	1.2	50	1483	trench	65

the abundance, this gives rise to a high flux of secondary neutrons traveling vast distances in the atmosphere. The peak of neutron intensity occurs at about 10–25 km, which is critical for avionic applications, being the altitude of many commercial airplane flights [21]. Below, there is a net loss of total particles in the cascades, having a flux which drops two orders of magnitude at sea level, with a neutron flux of less than 25 n/(cm²h) for energies higher than 1 MeV [22]. Data centers and the Si power electronics community have reported failures and upsets at sea level [24]–[27]. In addition, due to the exponential increase of neutron flux with increasing altitudes, problems can be encountered for applications at higher altitudes, for example, on a mountain top [23].

Furthermore, neutrons can cause issues for electronic systems installed in high-energy accelerators, such as the Large Hadron Collider (LHC) complex and its future upgrade High Luminosity LHC (HL-LHC) at CERN, Geneva, Switzerland [28]. Here, commercial SiC power MOSFETs have been considered for the design of a prototype inductive adder (IA) to be used as a pulse generator for the injection kicker magnets [5], [6].

The physics of neutron-induced SEB in SiC power devices has been previously studied, and an explanation for this destructive effect was suggested in [7]. Although neutrons are non-ionizing particles, the recoiling atoms, generated from their elastic or inelastic scattering with the lattice atoms, can indirectly give rise to ionization and create a large number of electron and hole (e–h) pairs along their trajectories. This event is followed by a hole impact ionization with associated multiplication factors and a consequent thermal transient and excessive lattice temperatures. This leads to local lattice sublimation and formation of voids, resulting in the loss of device blocking ability, hence a destructive failure. A schematic of the neutron interaction with the 4H-SiC lattice is shown in Fig. 1. Finally, it was reported that no consistent differences have been observed in the SEB tolerance for SiC MOSFETs and SiC diodes [8]. This supports the hypothesis that the conventional mechanisms underlying SEB in Si MOSFETs, such as parasitic bipolar junction transistor (BJT) and tunneling-assisted avalanche multiplication mechanisms [29], may be suppressed in SiC devices, where the current gain of the parasitic BJT is lower. Indeed, there is no similar parasitic BJT structure in the diode design.

In this work, we investigate the effect of neutron irradiation on different commercial SiC power MOSFETs produced

by different manufacturers. The devices were selected with three different types of designs: planar gate, trench gate, and double trench, where the last has a trench gate and a trench source [30]. The schematics of the three architectures are shown in Fig. 2. The radiation sensitivity is discussed for the different technologies. Experiments were performed at ChipIr, the beamline at the Rutherford Appleton Laboratory, Didcot, U.K. providing an atmospheric-like neutron environment. During irradiations, destructive failures were observed and the failure cross sections and failure-in-time (FIT) rates are presented for the tested references. In addition, from the post-irradiation analysis, the latent damage and the impact of gate rupture in planar and trench gate design are discussed, highlighting the differences among these device types and the dependence of the failure type on the technology. Finally, the results for the post-irradiation gate stress (PIGS), performed as recommended by the MIL-STD-750, test method 1080 [31], are also presented.

II. NEUTRON IRRADIATION EXPERIMENT

A. ChipIr Terrestrial Neutron Facility

ChipIr is a beamline built at the second target station (TS2) of the ISIS spallation source at the Rutherford Appleton Laboratory [32]–[34]. The facility is specifically tailored for testing radiation effects on electronic components and systems. The beamline design is optimized to mimic the atmospheric neutron spectrum (up to 800 MeV) with an acceleration factor of up to 10⁹ for ground-level applications. The neutrons delivered to the ChipIr facility are emitted from the spallation of high-energy protons with a tungsten target (i.e., 800-MeV protons extracted from the synchrotron with a beam current of 40 μ A and pulsed at 10 Hz). The neutrons are delivered to ChipIr according to the time structure of the ISIS source, i.e., in 10-Hz pulses, with two 70-ns-wide bunches separated 360 ns apart. A silicon diode, placed in front of the testing position, measures the energy distribution of single pulses. This is used to retrieve the neutron fluence at the device under test (DUT) location knowing the detection efficiency and, by means of a correction factor function of the distance between the diode and the DUT position, which takes into account the beam divergence. During the test campaign, the measured flux of neutrons above 10 MeV was 5.6×10^6 cm⁻²s⁻¹ at the testing position. A collimator system allows for selecting beams of different sizes. For the current experiment, a beam size of 10 \times 10 cm² was used.

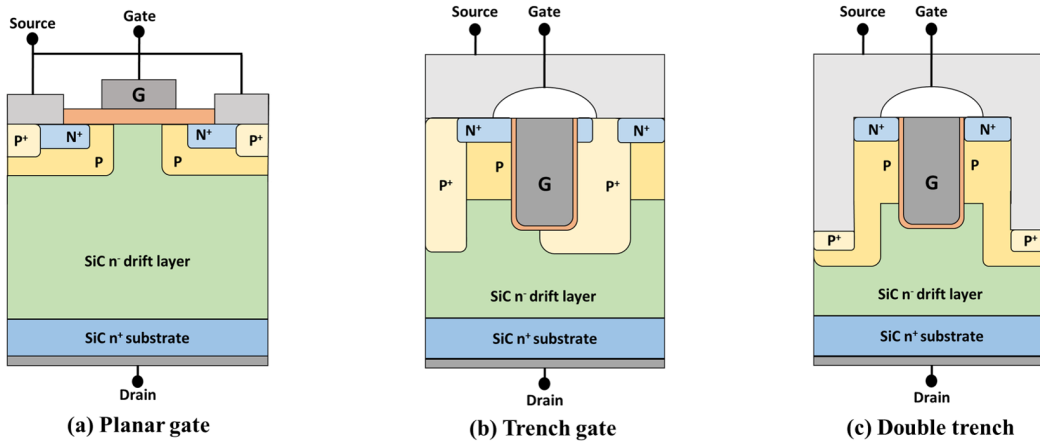


Fig. 2. Schematics of the three architectures of SiC power MOSFETs tested in this work. (a) Planar gate, (b) trench gate from Infineon, and (c) double trench (a trench source and a trench gate) from Rohm. Image remake after the original from Siemieniec *et al.* [30].

B. Experimental Method

The aim of this study is to investigate the effect of atmospheric-like neutrons on different commercial SiC MOSFET technologies. Accelerated testing of SEB by using terrestrial neutrons was performed. The obtained data were used to calculate the effect cross sections and FIT rates at ground level. In addition, the devices that did not exhibit destructive failure during exposure were characterized, and their operational reliability was studied.

Several samples were selected from the commercially available SiC VD-MOSFET technologies. The references and the corresponding technical information are listed in Table I. All the devices are rated for 1.2 kV, and they are mounted in a TO-247 package. The devices were irradiated in their original packaging. The first three devices were selected with similar values of $R_{DS(ON)}$ among them, and the same was done for the last two devices. The references were selected with different designs: planar, trench, and double trench. In particular, the DUTs from Infineon have a trench gate structure [35], whereas the Rohm have a double trench design, with a trench gate and a trench source. For the trench gate devices, the channel is formed vertically, which allows the vertical flow of current while reducing $R_{DS(ON)}$ [36]. All the other references have a planar gate structure.

The test setup was designed following the military standard specifications (MIL-STD-750E M1080.1) [31]. Each test board can host a maximum of 12 devices in parallel. A schematic layout of the setup is presented in Fig. 3, where two DUTs are illustrated for brevity. Two boards were stacked to test up to 24 DUTs for each run. They were installed at a distance of 58 and 76 cm from the beam aperture, respectively. The attenuation of the neutron beam in the first board was estimated to be negligible for the material used in the tested boards [37]. Two Keithley Source Measurement Unit (SMU) model 2410 s (one channel, up to 1100 V), one for each board, were used to bias the drain and to monitor the total leakage currents as a sum of all devices. The gates were grounded directly on the board. A stiffening capacitor of 10 nF was installed between the drain and the ground for each DUT, in order to supply sufficient amount of charge during a destruc-

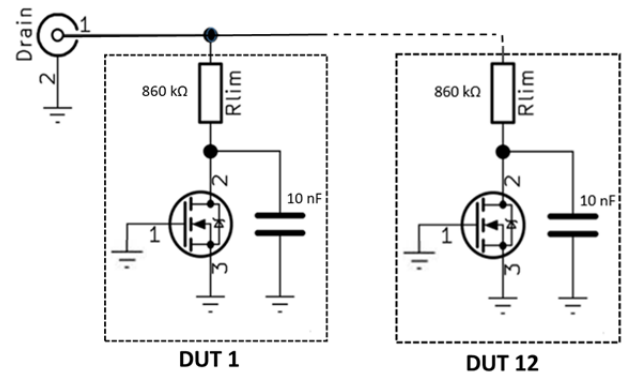


Fig. 3. Schematic layout of the setup. Only two DUTs out of 12 hosted by a single board are illustrated here for brevity.

tive event. Moreover, it also limited the momentary voltage drop at the SMU output during current transients. The devices were connected in parallel to the high voltage, but each of them had an individual current-limiting resistor of 860 kΩ between the drain and the SMU output. This guaranteed the isolation of the device after a failure and the continuous application of high voltage to all other devices. Each step increase in the total current measured by the SMU was accounted as a failure ($\Delta I_{DS} = 1.27$ mA). This value corresponds to a short circuit on the DUT, having the total voltage applied across the protection resistor. In Fig. 4, an example of the online measurements recorded during an exposure run is shown. The results are presented for Rohm SCT3030KL devices exposed at 1100 V. Here, the measured drain current was divided by the failure step size ($\Delta I_{DS} = 1.27$ mA) in order to highlight the number of failures during the run.

For each reference, three irradiations were performed on pristine devices at V_{DS} of 1100, 976, and 846 V, which are $\sim 92\%$, $\sim 81\%$, and 72% of the maximum rated voltage (1.2 kV), respectively. During irradiation, $V_{GS} = 0$ V to keep the device in OFF-state. The gate current was not monitored during the run. The test was stopped when 50%–70% of devices failed or when a fluence of 2.8×10^{10} n/cm² was reached.

Some of the DUTs were characterized after the irradiation using a Keithley Parametric Curve Tracer PCT-4B in order to

TABLE II
FAILURE ANALYSIS

Reference	Man.	V_{DS} irradiation [V]	β	η [n/cm^2]	Failed / Total DUT	σ_{SEB} [cm^2]	MTBF [h]
C2M0025120D	Cree/ Wolfspeed	1100	0.70	3.31×10^7	6 / 13	2.39×10^{-8}	4.18×10^7
		976	0.67	9.43×10^7	11 / 20	8.04×10^{-9}	1.24×10^8
		846	0.97	1.47×10^9	8 / 18	6.71×10^{-10}	1.49×10^9
SCT3030KL	ROHM	1100	1.14	2.24×10^9	9 / 24	4.69×10^{-10}	2.13×10^9
		976	4.02	2.24×10^9	2 / 24	4.93×10^{-10}	2.03×10^9
MSC025SMA120B	Microsemi	1100	1.54	8.12×10^5	13 / 13	1.37×10^{-6}	7.31×10^5
		976	1.12	1.31×10^7	11 / 15	7.96×10^{-8}	1.26×10^7
		846	0.85	1.34×10^8	13 / 22	6.85×10^{-9}	1.46×10^8
SCTWA50N120	ST-Micr.	1100	0.85	4.33×10^6	19 / 20	2.13×10^{-7}	4.69×10^6
		976	1.05	1.13×10^7	17 / 22	9.06×10^{-8}	1.10×10^7
		846	1.04	9.32×10^7	15 / 24	1.09×10^{-8}	9.15×10^7
IMW120R090M1H	Infineon	1100	0.91	6.41×10^7	14 / 17	1.50×10^{-8}	6.67×10^7
		976	0.82	5.83×10^8	16 / 24	1.54×10^{-9}	6.49×10^8
		846	0.93	2.60×10^9	8 / 24	3.73×10^{-10}	2.68×10^9

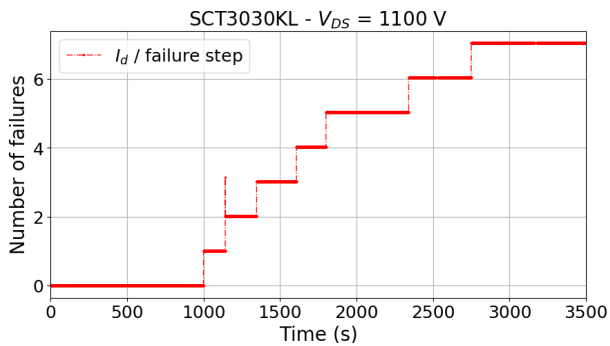


Fig. 4. Example of online measurement for Rohm devices (SCT3030KL) exposed at 1100 V. The drain current measured during the exposure is divided by the failure step size in order to highlight the number of failures during the run.

investigate the radiation-induced damage. In addition, breakdown voltage (BV_{DSS}) measurements were conducted using a Keithley SMU 2657A on the drain and a Keithley SMU 2636B on the gate and the source terminals. For a pristine device, BV_{DSS} is the voltage at which the reverse-biased body-drift diode breaks down causing significant current to flow between the source and the drain due to the avalanche multiplication process.

III. EXPERIMENTAL RESULTS

A. Weibull Distribution Analysis and FIT Rates

In order to calculate the SEB cross sections and the FIT rates, reliability parameters were determined using a standard two-parameter Weibull distribution [23]. The cumulative fraction of failed devices was calculated as a function of the neutron fluence; a two-parameter Weibull distribution was fit to the data using a maximum likelihood estimation (MLE) method [38]. Two parameters were extracted from this analysis: β , called the shape parameter, which is an indicator of the failure mechanism, and η , which is the scale parameter. Weibull distributions with $\beta < 1$ have an early-life failure, which decreases with time, while distributions with $\beta > 1$ have a failure rate that increases with time, also known as wear-out failures. For stochastic neutron failures $\beta = 1$ is

expected, as representative of random events. The mean time between failures (MTBFs) and SEB cross sections (σ_{SEB}) were calculated as follows:

$$\begin{aligned}
 \text{MTBF} &= \eta \times \Gamma\left(1 + \frac{1}{\beta}\right) \quad \text{when } \beta \neq 1 \\
 \text{MTBF} &= \eta \quad \text{when } \beta = 1 \\
 \sigma_{SEB} &= \frac{1}{\text{MTBF}}. \tag{1}
 \end{aligned}$$

The error bars were calculated considering a Poisson distribution dominated by the count statistics. The uncertainty over the fluence was considered negligible with respect to the number of events. The upper and lower limits were calculated as in the following equation, where N_{low} and N_{high} were obtained from the chi-square distribution with a confidence level of 95%:

$$\begin{aligned}
 \text{Err}_{high} &= \frac{N_{high}}{N_{SEB} * \text{MTBF}} \\
 \text{Err}_{low} &= \frac{N_{low}}{N_{SEB} * \text{MTBF}}. \tag{2}
 \end{aligned}$$

The FIT rates were calculated considering 10^9 h of operations and a cosmic-ray-induced neutron flux of $13 \text{ n}/(\text{cm}^2 \cdot \text{h})$ for energies above 10 MeV (reference conditions at sea level in NYC from JEDEC JESD89A standard). The same conversion factor was also used for the error bars as described above for cross sections.

In Table II, the parameters extracted from the analysis are listed for the tested references. In the case of Rohm, the tests were performed only at 1100 V and 976 V. In some runs, multiple SEBs were observed at the same time. For the analysis, they were considered as a single event, in order to assure the independence between the SEB events. Therefore, the total number of tested DUTs was reduced.

The failure cross sections are shown in Fig. 5(a) as a function of the bias during irradiation. In Fig. 5(b), the FIT rates are shown for the tested references, while in Fig. 5(c), the FIT rates are normalized with the active area and scaled by the avalanche breakdown voltage, such that a ratio of 1 would indicate that the critical field was reached. This approach was suggested and previously discussed in [9]. A common trend

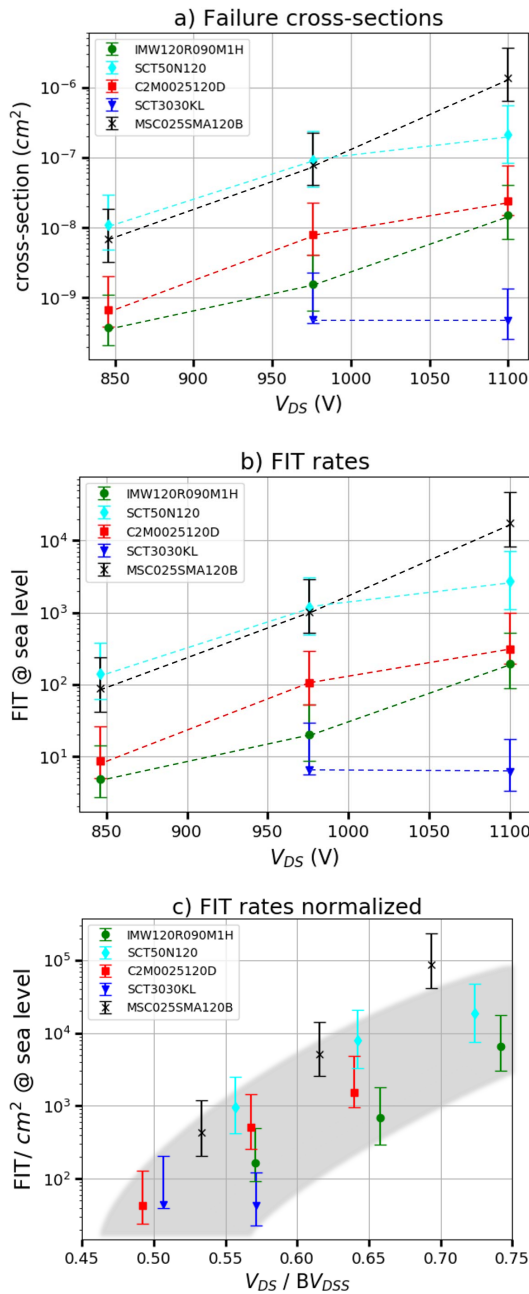


Fig. 5. (a) Failure cross sections of SiC MOSFETs from different suppliers as a function of the bias during the terrestrial neutron irradiations. (b) FIT rates for 10^9 h of operation. (c) FIT rates scaled by avalanche voltage and normalized with the active area.

is observed for all the devices and highlighted by the gray shadow. The trench MOSFETs (i.e., IMW120R090M1H and SCT3030KL) appear to have lower FIT rates if compared to the planar architecture. In particular, the double-trench device (SCT3030KL), which has the highest avalanche breakdown voltage, has the best performance.

B. Postirradiation Measurements: Breakdown Voltage

Postirradiation measurements were performed for some devices, which showed more or less severe effects depending on the technology. In this and Sections III-C and III-D, the measurements are discussed for the three tested architectures:

planar gate from Cree/Wolfspeed (i.e., C2M0025120D), trench gate from Infineon (i.e., IMW120R090M1H), and double trench from Rohm (i.e., SCT3030KL). As an example, the results are compared for the references tested at 976 V. BV_{DSS} measurements of the irradiated devices were performed at $V_{GS} = 0$ V and stopped at V_{DS} corresponding to $I_D = 1.00$ mA, which is defined as the breakdown voltage. At this current level, the device is still protected from a permanent breakdown of the body diode. Three different responses were identified for all the studied references: i) no damage observed with respect to a pristine device; ii) partial degradation of the device, which exhibited higher gate and drain leakage currents; and iii) ohmic trend of the leakage current caused by SEB. Examples of the leakage currents (I_D , I_G , and I_S) are reported as a function of the drain–source bias (V_{DS}) for the three references in Fig. 6. The top and the bottom panels show, respectively, the measurements for (i) and (ii) scenarios described above. A measurement of a pristine device for each reference is given in gray for comparison. In Fig. 6(a)–(c), the measurements are all in the same range as the pristine device, and the small differences observed are caused by part-to-part variations (i.e., the pristine device is not the same part as the irradiated one, but belongs to the same lot). For these devices, no damage was induced by the neutron exposure and no leakage current increase is observed, neither degradation of the blocking capability of the MOSFETs. Differently, a clear degradation was induced by the neutron exposure in the devices reported in Fig. 6(d)–(f). The leakage currents are orders of magnitudes higher with respect to the pristine level for all the three devices; however, the current paths (drain-to-gate versus drain-to-source contributions) differ among them.

Finally, the measurements for (iii) are not reported, but from the ohmic trend of the leakage current, it was concluded that the devices failed through an SEB during the exposure.

C. Postirradiation Measurements: Gate Damage

In order to investigate the different leakage path observed for (ii), I_D – V_{GS} and I_G – V_{GS} measurements were performed at $V_{DS} = 1$ V. The results are presented in Fig. 7, which shows that the gate oxide is still operable for the planar device (C2M0025120D) and the channel is still controlled by the gate voltage, but the gate leakage is higher with respect to the pristine level. The device exhibits a partial gate rupture with very high gate and drain leakage current and a gate–drain current path. This effect is similar to the degradation induced by heavy-ion exposure (i.e., SELC), previously reported in [18] and [19]. Conversely, repeating the measurement for the double-trench (SCT3030KL) and the trench (IMW120R090M1H) devices, the gate oxide was found to be heavily damaged and not operable anymore. Indeed, the channel is in OFF-state for these devices and no positive drain current flows. From these observations, it was concluded that the damage in the trench devices has the signature of a complete gate rupture.

D. Latent Damage: PIGS Test

Even though a device may not show any measurable damage during irradiation, as for category (i), the integrity of its

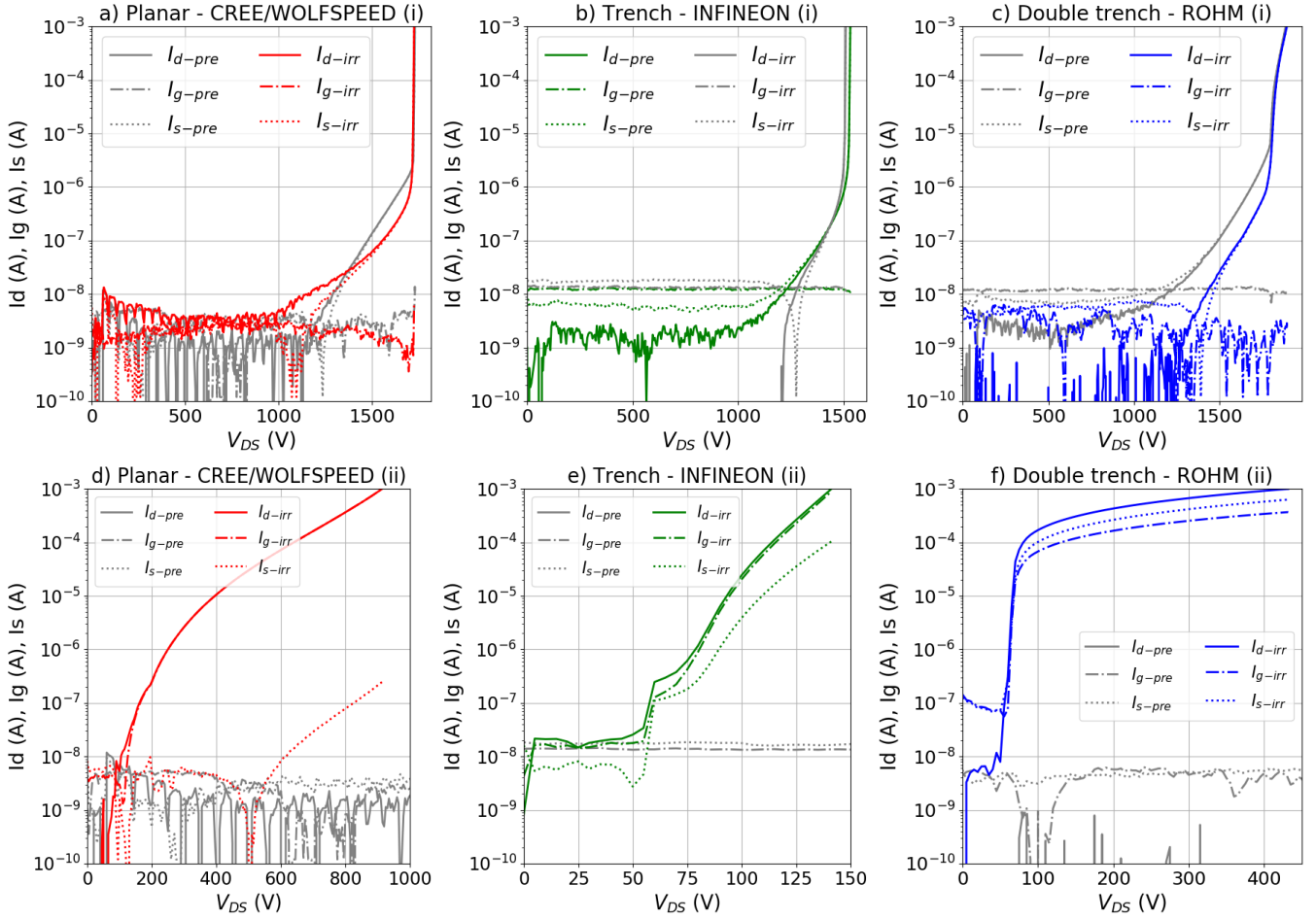


Fig. 6. Different responses were observed in the devices exposed to neutrons: i) no failure observed and no damage with respect to a pristine device, as in (a), (b), and (c) and ii) no failure observed, but partial degradation of the device, as in (d), (e), and (f). The measurements of the leakage currents (I_D , I_G , and I_S) were performed at $V_{GS} = 0V$ and with a maximum I_D current of 1 mA.

gate oxide might be affected. In order to study the effect of latent damage on the gate oxide integrity and on the blocking capability, breakdown voltage measurements were repeated after applying positive and negative voltage bias at the gate oxide, following the PIGS test as recommended in MIL-STD-750, test method 1080 [31]. V_{GS} was first swept positively up to the rated value for each reference (i.e., +15 V for Cree/Wolfspeed, +18 V for Infineon, and +22 V for Rohm) or until a leakage current of 1 mA was measured. Second, a $V_{GS} = -5 V$ was then applied at the gate oxide. The results are shown in Fig. 8(a)–(c) for the three devices discussed before in Fig. 6(a)–(c), respectively, which did not exhibit any measurable damage after the exposure (i). No difference was observed in the breakdown point and in the leakage currents after these cycles. The small differences in the gate leakage current might be due to the instrument sensitivity. Hence, these devices are operable after the neutron irradiation, the leakage current is still within the specification (i.e., $I_G < 100$ nA), and no latent damage is observed after applying the gate bias.

However, for the degraded device (ii) previously presented in Fig. 6(d), after the stress at negative V_{GS} , I_S decreased, meaning that higher current is flowing to the drain–gate path, rather than into the source pad, as shown in Fig. 8(d). This is evidence of an increased gate damage induced by the negative gate bias.

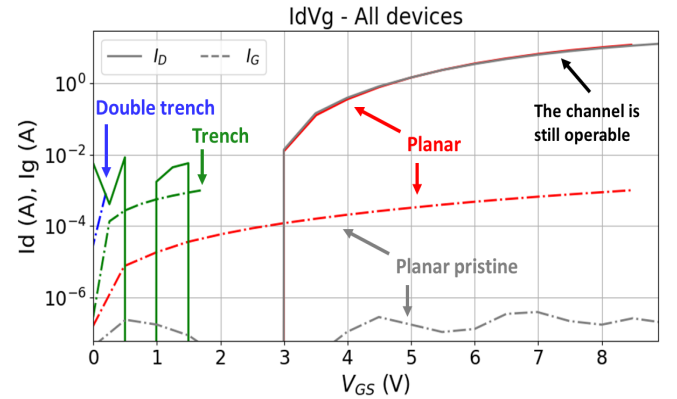


Fig. 7. I_D – V_{GS} and I_G – V_{GS} measurements performed at $V_{DS} = 1V$. The gate oxide is still operable for the planar Cree/Wolfspeed device (C2M0025120D) and the channel is still controlled by the gate voltage. Conversely, the gate oxide is heavily damaged and not operable anymore for the trench and double-trench structures.

IV. DISCUSSION

From the results presented, three different scenarios were commonly observed for the different architectures analyzed. Considering the FIT normalized with the active area and scaled by the breakdown voltage, the trench devices showed a better performance to SEB with respect to the planar ones, with the double-trench architecture as the most robust. However, part

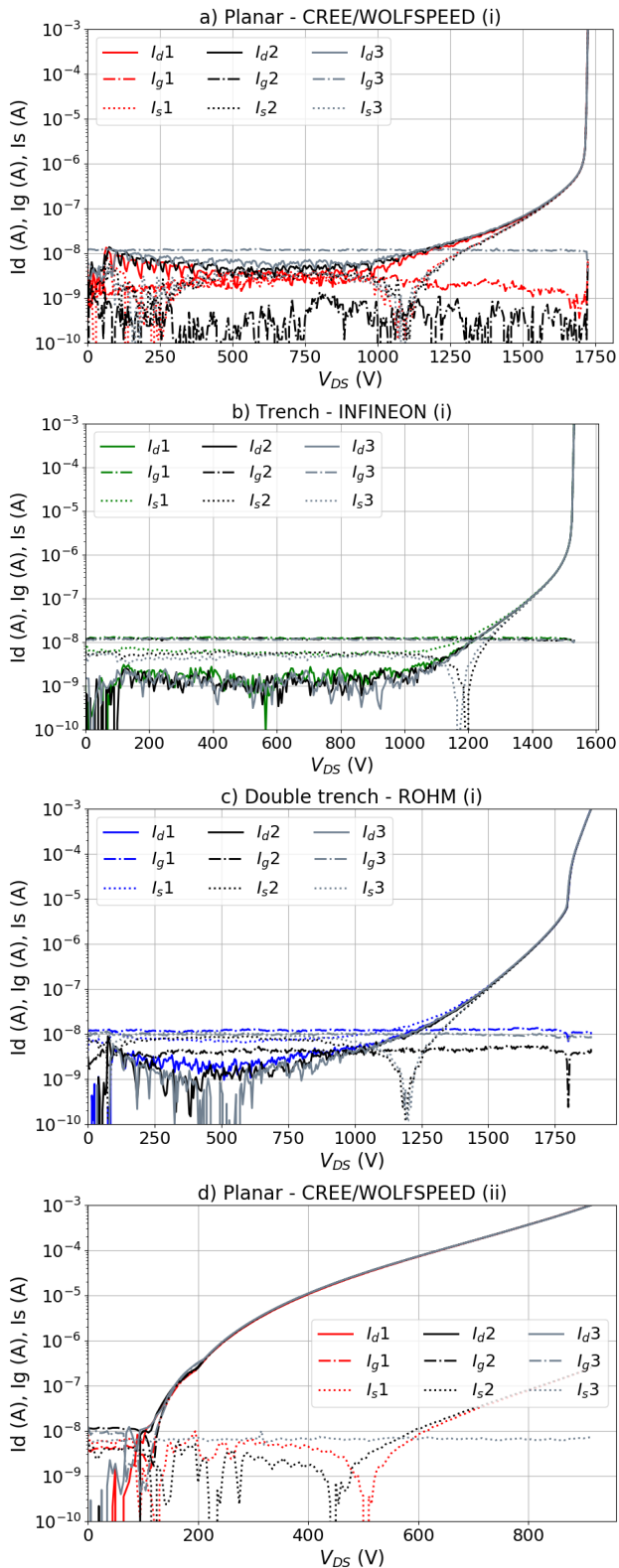


Fig. 8. Breakdown voltage measurements after the PIGS test. The results are reported for (a) planar, (b) trench, and (c) double-trench DUTs, which did not show any damage during the exposure (i), and for (d) planar DUT which was partially degraded (ii). The first cycle reports the measurement just after the irradiation, while the second and the third represent the measurements repeated after applying a positive V_{GS} up to the rated voltage and a negative V_{GS} of -5 V, respectively.

of the trench and double-trench devices exhibited a complete gate rupture. Conversely, a partial gate rupture was observed

for the planar reference analyzed, which exhibited a current leakage path between the gate and the drain as previously observed for planar gate devices suffering from SELC after heavy-ion irradiation. In addition, for the device with the gate partially ruptured, the gate damage increased after the PIGS test, which was already reported for devices suffering from SELC after heavy-ion experiments [39].

A model for an enhanced gate current associated with a leakage was previously presented for Si devices and heavy-ion irradiation. It states that the oxide defects from displacement damage caused by the ions create a significant number of damage sites at which there is a reduced potential barrier, permitting the tunneling of electrons from trapping sites in the oxide into the conduction band [40]. Similarly, a model for early defects in SiO_2/SiC was discussed in [41] and attributed to the presence of defects in the oxide bulk. It is hypothesized that, through displacement damage, neutrons are inducing defects in the gate oxide, which are responsible for the increased gate leakage current. Furthermore, the density and distribution of oxide defects in a pristine device depend on the oxide process and can be considered as a by-product of the SiO_2 oxide growth on SiC, and therefore different among devices produced by different manufacturers.

Finally, it should be noted that the setup used during the experiment was counting as a failure event all the devices whose I_D leakage current in OFF-state exceeded 1.27 mA. Therefore, the FITs and the failure cross section analysis include both the failure mechanism indicated as SEB (iii) and degradation with partial or complete gate rupture (ii), with the latter also considered not operable from an application point of view due to the very high leakage currents.

V. CONCLUSION

Results from accelerated terrestrial neutron experiments were presented for different commercial SiC technologies with planar, trench, and double-trench architectures.

Different failure mechanisms were observed from the post-irradiation analysis of the irradiated devices, and three different responses were commonly identified for each of the three architectures: (i) no damage observed with respect to a pristine device, (ii) partial degradation of the device, which exhibited high leakage currents, and (iii) SEB (i.e., ohmic trend of the leakage current). Categories (ii) and (iii) were considered failed devices from an application point of view. Failure cross sections and FIT rates were calculated for these devices. MOSFETs with a trench structure appear to be less sensitive to neutron-induced failures with respect to the planar ones. The double trench architecture, which also has the higher breakdown voltage, was observed to be the most robust.

Examples were reported and discussed for the degraded devices (ii) and the impact of gate rupture was discussed for the three designs. The planar-gate architecture exhibited a partial gate rupture mechanism, probably induced by displacement damage and characterized by very high leakage currents with a gate-drain current path. This effect was observed to be similar to the SELC degradation induced by heavy ions, already discussed for the same reference, but reported here for neutron irradiation. The trench and double-trench

architectures, instead, appeared to be more sensitive to a complete gate rupture.

However, it should be clearly stated that the experiments were performed using a specific device type from each manufacturer. Both the design as well as the resulting efficient carrier concentration in the specific areas will vary between device types and generation from the same manufacturer; therefore, the results cannot be extrapolated to all SiC power devices without further analysis.

REFERENCES

- [1] J. A. Cooper, M. R. Melloch, R. Singh, A. Agarwal, and J. W. Palmour, "Status and prospects for SiC power MOSFETs," *IEEE Trans. Electron Devices*, vol. 49, no. 4, pp. 658–664, Apr. 2002.
- [2] H. J. van Daal, C. A. A. J. Greebe, W. F. Knippenberg, and H. J. Vink, "Investigation on silicon carbide," *J. Appl. Phys.*, vol. 32, no. 10, pp. 2225–2233, Oct. 1961.
- [3] K. Shenai, K. F. Galloway, and R. D. Schrimpf, "The effects of space radiation exposure on power MOSFETs: A review," *Int. J. High Speed Electron. Syst.*, vol. 14, no. 2, pp. 445–463, Jun. 2004.
- [4] K. F. Galloway *et al.*, "Failure estimates for SiC power MOSFETs in space electronics," *Aerospace*, vol. 5, no. 3, p. 67, Jun. 2018.
- [5] D. Woog, M. J. Barnes, L. Ducimetière, J. Holma, and T. Kramer, "Design of an inductive adder for the FCC injection kicker pulse generator," *J. Phys., Conf. Ser.*, vol. 874, Jul. 2017, Art. no. 012096.
- [6] L. M. Redondo, A. Kandratsyev, and M. J. Barnes, "Marx generator prototype for kicker magnets based on SiC MOSFETs," *IEEE Trans. Plasma Sci.*, vol. 46, no. 10, pp. 3334–3339, Oct. 2018.
- [7] A. Akturk *et al.*, "Terrestrial neutron-induced failures in silicon carbide power MOSFETs and diodes," *IEEE Trans. Nucl. Sci.*, vol. 65, no. 6, pp. 1248–1254, Jun. 2018.
- [8] H. Asai *et al.*, "Tolerance against terrestrial neutron-induced single-event burnout in SiC MOSFETs," *IEEE Trans. Nucl. Sci.*, vol. 61, no. 6, pp. 3109–3114, Dec. 2014.
- [9] D. J. Lichtenwalner *et al.*, "Reliability of SiC power devices against cosmic ray neutron single-event burnout," *Mater. Sci. Forum*, vol. 924, pp. 559–562, Jun. 2018.
- [10] A. Akturk, R. Wilkins, J. McGarrity, and B. Gersey, "Single event effects in Si and SiC power MOSFETs due to terrestrial neutrons," *IEEE Trans. Nucl. Sci.*, vol. 64, no. 1, pp. 529–535, Jan. 2017.
- [11] A. Griffoni *et al.*, "Neutron-induced failure in super-junction, IGBT, and SiC power devices," *IEEE Trans. Nucl. Sci.*, vol. 59, no. 4, pp. 866–871, Mar. 2012.
- [12] A. Akturk, J. M. McGarrity, R. Wilkins, A. Markowski, and B. Cusack, "Space and terrestrial radiation response of silicon carbide power MOSFETs," in *Proc. IEEE Radiat. Effects Data Workshop (REDW)*, New Orleans, LA, USA, Jul. 2017, pp. 237–241.
- [13] A. Akturk *et al.*, "The effects of radiation on the terrestrial operation of SiC MOSFETs," in *Proc. IEEE Int. Rel. Phys. Symp. (IRPS)*, Burlingame, CA, USA, Mar. 2018, Art. no. 2B.1.
- [14] A. Akturk *et al.*, "Predicting cosmic ray-induced failures in silicon carbide power devices," *IEEE Trans. Nucl. Sci.*, vol. 66, no. 7, pp. 1828–1832, Jul. 2019.
- [15] K. Niskanen *et al.*, "Impact of electrical stress and neutron irradiation on reliability of silicon carbide power MOSFET," *IEEE Trans. Nucl. Sci.*, vol. 67, no. 7, pp. 1365–1373, Jul. 2020.
- [16] A. Javanainen *et al.*, "Heavy ion induced degradation in SiC Schottky diodes: Bias and energy deposition dependence," *IEEE Trans. Nucl. Sci.*, vol. 64, no. 1, pp. 415–420, Jan. 2017.
- [17] E. Mizuta, S. Kuboyama, H. Abe, Y. Iwata, and T. Tamura, "Investigation of single-event damages on silicon carbide (SiC) power MOSFETs," *IEEE Trans. Nucl. Sci.*, vol. 61, no. 4, pp. 1924–1928, Aug. 2014.
- [18] D. R. Ball *et al.*, "Ion-induced energy pulse mechanism for single-event burnout in high-voltage SiC power MOSFETs and junction barrier Schottky diodes," *IEEE Trans. Nucl. Sci.*, vol. 67, no. 1, pp. 22–28, Jan. 2020.
- [19] C. Martinella *et al.*, "Current transport mechanism for heavy-ion degraded SiC MOSFETs," *IEEE Trans. Nucl. Sci.*, vol. 66, no. 7, pp. 1702–1709, Jul. 2019.
- [20] C. Martinella *et al.*, "Heavy-ion microbeam studies of single-event leakage current mechanism in SiC VD-MOSFETs," *IEEE Trans. Nucl. Sci.*, vol. 67, no. 7, pp. 1381–1389, Jul. 2020.
- [21] M. Xapsos, "A brief history of space climatology: From the big bang to the present," *IEEE Trans. Nucl. Sci.*, vol. 66, no. 1, pp. 17–37, Jan. 2019.
- [22] J. F. Ziegler, "Terrestrial cosmic rays," *IBM J. Res. Dev.*, vol. 40, no. 1, pp. 19–39, Jan. 1996.
- [23] F. D. Bauer, "Accurate analytical modelling of cosmic ray induced failure rates of power semiconductor devices," *Solid-State Electron.*, vol. 53, no. 6, pp. 584–589, Jun. 2009.
- [24] S. E. Michalak, K. W. Harris, N. W. Hengartner, B. E. Takala, and S. A. Wender, "Predicting the number of fatal soft errors in Los Alamos National Laboratory's ASC Q supercomputer," *IEEE Trans. Device Mater. Rel.*, vol. 5, no. 3, pp. 329–335, Sep. 2005.
- [25] D. L. Oberg, J. L. Wert, E. Normand, P. P. Majewski, and S. A. Wender, "First observations of power MOSFET burnout with high energy neutrons," *IEEE Trans. Nucl. Sci.*, vol. 43, no. 6, pp. 2913–2920, Dec. 1996.
- [26] R. Sheehy, J. Dekter, and N. Machin, "Sea level failures of power MOSFETs displaying characteristics of cosmic radiation effects," in *Proc. IEEE 33rd Annu. IEEE Power Electron. Specialists Conf.*, Cairns, QLD, Australia, Jun. 2002, pp. 445–463.
- [27] E. H. Ibe, *Terrestrial Radiation Effects in ULSI Devices and Electronic Systems*. Singapore: Wiley, 2015.
- [28] R. G. Alia *et al.*, "LHC and HL-LHC: Present and future radiation environment in the high-luminosity collision points and RHA implications," *IEEE Trans. Nucl. Sci.*, vol. 65, no. 1, pp. 448–456, Jan. 2018.
- [29] T. Shoji *et al.*, "Reliability design for neutron induced single-event burnout of IGBT," *IEEE Trans. Ind. Appl.*, vol. 131, no. 8, pp. 992–999, Aug. 2011.
- [30] R. Siemieniec *et al.*, "A SiC trench MOSFET concept offering improved channel mobility and high reliability," in *Proc. 19th Eur. Conf. Power Electron. Appl. (EPE ECCE Eur.)*, Warsaw, Poland, Sep. 2017, Art. no. P-1.
- [31] *Single-Event Burnout and Single-Event Gate Rupture, Method 1080.1 in Test Methods for Semiconductor Devices*, Standard MIL-STD-750-1, Jan. 2012.
- [32] C. Cazzaniga and C. D. Frost, "Progress of the scientific commissioning of a fast neutron beamline for chip irradiation," *J. Phys., Conf. Ser.*, vol. 1021, Jun. 2018, Art. no. 012037.
- [33] C. Cazzaniga, M. Bagatin, S. Gerardin, A. Costantino, and C. D. Frost, "First tests of a new facility for device-level, board-level and system-level neutron irradiation of microelectronics," *IEEE Trans. Emerg. Top. Comput.*, vol. 9, no. 1, pp. 104–108, Jan./Mar. 2021.
- [34] C. Cazzaniga, R. G. Alia, M. Kastriotou, M. Cecchetto, P. Fernandez-Martinez, and C. D. Frost, "Study of the deposited energy spectra in silicon by high-energy neutron and mixed fields," *IEEE Trans. Nucl. Sci.*, vol. 67, no. 1, pp. 175–180, Jan. 2020.
- [35] D. Peters *et al.*, "Performance and ruggedness of 1200V SiC—Trench—MOSFET," in *Proc. 29th Int. Symp. Power Semiconductor Devices IC's (ISPSD)*, Sapporo, Japan, May 2017, pp. 239–242.
- [36] R. K. Williams, M. N. Darwish, R. A. Blanchard, R. Siemieniec, P. Rutter, and Y. Kawaguchi, "The trench power MOSFET: Part I—History, technology, and prospects," *IEEE Trans. Electron Devices*, vol. 64, no. 3, pp. 674–691, Mar. 2017.
- [37] C. Cazzaniga, B. Bhuva, M. Bagatin, S. Gerardin, N. Marchese, and C. D. Frost, "Atmospheric-like neutron attenuation during accelerated neutron testing with multiple printed circuit boards," *IEEE Trans. Nucl. Sci.*, vol. 65, no. 8, pp. 1830–1834, Aug. 2018.
- [38] *Reliability PyPI*. Accessed: Jan. 3, 2021. [Online]. Available: <https://pypi.org/project/reliability/>
- [39] C. Abbate, G. Busatto, D. Tedesco, A. Sansverino, F. Velardi, and J. Wyss, "Gate damages induced in SiC power MOSFETs during heavy-ion irradiation—Part I," *IEEE Trans. Electron Devices*, vol. 66, no. 10, pp. 4243–4250, Oct. 2019.
- [40] L. Scheick, L. Edmonds, L. Selva, and Y. Chen, "Current leakage evolution in partially gate ruptured power MOSFETs," *IEEE Trans. Nucl. Sci.*, vol. 55, no. 4, pp. 2366–2375, Aug. 2008.
- [41] Z. Chbili *et al.*, "Modeling early breakdown failures of gate oxide in SiC power MOSFETs," *IEEE Trans. Electron Devices*, vol. 63, no. 9, pp. 3605–3613, Sep. 2016.